

Reports

Possible Fossil Lunar Magnetism Inferred from Satellite Data

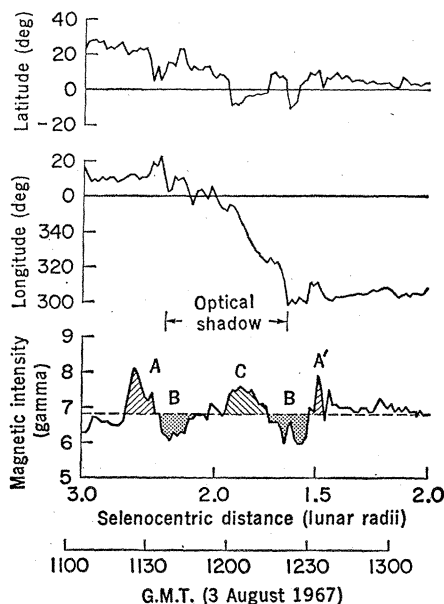
Abstract. Magnetization of selected nonmare areas, principally on the moon's far side, is inferred from positive disturbances in the magnitude of the magnetic field exterior to the magnetic signature of the lunar cavity observed in magnetometer data from the lunar orbiter Explorer 35. A less favored model for the field perturbations involves variations in the thickness of the low-conductivity crustal layer of the moon.

In conjunction with the diamagnetic solar wind cavity discovered behind the moon by the lunar orbiter Explorer 35 (1), there appear sporadic but persistent maxima in the magnitude of the interplanetary magnetic field adjacent to the rarefaction wave (2) which bounds the edges of the cavity. In this report lunar limb sources for the most prominent of these increases are assumed and a map of the lunar surface prepared under this assumption is presented. Most sources are located on the moon's far side, with most of them restricted to the highlands. The alternative mechanisms for an interaction between the solar wind and the limb, local surface magnetic fields, and variations in crustal conductivity are discussed. The term "limb" in this report refers to the solar wind limb, or the boundary of the moon's hemisphere struck by the undeflected solar plasma.

Figure 1 shows a magnetic signature displaying the cavity formed by the moon in the diamagnetic plasma of the solar wind (C), regions characterized by rarefaction waves (B), and a positive change in the magnitude of the magnetic field (A) of the sort discussed here. An increase in the magnitude of the magnetic field in the cavity interior (C) and the associated decreases of $\frac{1}{2}$ to 1 gamma (B) (1 gamma = 10^{-5} gauss) are frequently observed (1, 3). The isolated increase in the magnetic field of more than 1 gamma seen at 1125 G.M.T. prior to entry of the satellite into the optical shadow of the moon (A) is a feature that is observed infrequently.

About 100 of the most pronounced cases of increased amplitude, almost all restricted to the amplitude range of 0.8 to 3.5 gamma, are included here. These correspond to 7.4 percent of all

available shadow edges examined, excluding data gaps, during the period from July 1967 to May 1969. Additional data to July 1970 have been examined but are not discussed here. Marked changes in the direction of the magnetic field are not usually associated with these perturbations but variations in the bulk flow direction of the plasma have been reported to accompany the change in amplitude (4). Less distinct increases (generally < 0.8 gamma), whose origins are difficult to determine, are observed about 50 percent of the time (3, 4). The brief increase in the magnitude of the field at 1233 G.M.T. (A') is not counted in this study. (The probability that the chosen peaks are false falls in the range between 10^{-1} and 10^{-3} ; A' is an example with this probability $> 10^{-1}$ that is not chosen.) The amplitudes of the smallest maxima in the magnitude of the magnetic field considered here



are somewhat less than that of moderate natural fluctuations in the interplanetary field that are sometimes observed. Noisy fields are reported as nulls because the perturbations may be masked. Consequently, the selection of maxima is slightly biased toward times of quiet interplanetary fields. The position of the field increases (invariably lying outside of the rarefaction wave and in the free-stream solar wind) suggests a wave structure standing in the wind, thus implying a supersonic speed (Mach angle, $\sim 7^\circ$). Earlier reports (3-5) suggest the formation of an occasional weak standing shock wave arising from grazing interaction of the solar wind and terminator.

The approximate positions on the lunar surface where an interaction between the solar wind and the limb would originate have been located by the following procedure. For 18 cases where data on the vector velocity of the bulk plasma have been used, the position in orbit of the perturbation is projected in the direction opposite to solar wind flow; for the remaining ~ 80 percent of the cases an average aberration angle of 4° is assumed for the solar wind flow in making the projection. The positions on the lunar surface nearest to the rays of projection are noted on a Mercator map displaying both hemispheres. The result is shown in Fig. 2 where the fractions of projected locations associated with exterior maxima are indicated in shaded areas, 15° wide in longitude and latitude. No source locations for exterior maxima are found in the polar regions (not shown in Fig. 2).

A preliminary estimate of the error associated with the position on the moon of perturbation sources is $\sim \pm 5^\circ$ in both longitude and latitude near the

Fig. 1. Sequence-average data from the Ames magnetometer aboard Explorer 35 (three sequences, 40 vector samples, 245.4 seconds), in solar ecliptic coordinates, that demonstrate a prominent isolated peak in the magnitude of the magnetic field at 1125 G.M.T. (A). This maximum is exterior to the diamagnetic cavity (C) that is bounded near the limits of the optical shadow. The latitude angle is that from the ecliptic plane to the field vector measured positive toward the north. The longitude angle is measured from the spacecraft-sun line to the projection onto the ecliptic plane of the vector, positive counterclockwise as viewed from the north. The dashed line gives the estimate of the magnitude of the background interplanetary magnetic field during this time.

equator for cases for which plasma data are not available, and $\sim \pm 1.5^\circ$ for cases with the value of the plasma vector velocity. Both estimates are based on the model described above.

The results plotted in Fig. 2 indicate that source locations in the highlands are strongly favored. This follows from the fact that the preferred locations of the sources are on the moon's far side, which is largely highland with few, if any, maria of the sort found on the near side. The probability that far-side locations are not favored, on the basis of a 2×2 contingency table of the observations given in Fig. 2 and the remaining cases for which no exterior maxima are seen, is $\ll 10^{-5}$. (This coarse test similarly suggests favored source locations when the surface is not sunlit.) Figure 2 shows that the largest concentration of locations, clearly observed on several separate occasions, lies near 20°S and 145°E on the far side of the moon. Other concentrations of sources are indicated in Table 1. The bias of locations near the lunar equator may be influenced by the extreme geometry when the Explorer satellite scans the polar regions. All regions of the moon are scanned during the period of these data as a result of the revolution of the earth-moon system about the sun together with the revolution of the moon about the earth, the skewed form of the orbit, and the precession of periselenae.

A more detailed analysis has been made of seven regions where source locations seem to be concentrated. In order of decreasing concentration, approximate selenographic coordinates of the centers of these regions and their areas are given in Table 1, together with the names of nearby lunar features and fractional numbers of observations showing anomalies. Each entry in Table 1 is based on at least three observations of exterior maxima. About one-third of the source locations lie outside of these seven regions. These observations suggest strongly that there is an intermittent interaction between the solar wind and the limb of the moon which depends primarily upon the particular selenographic position adjacent to the terminator at the time of the observation.

Permanent magnetic fields are known to exist on the lunar surface; a field of 38 ± 3 gamma was reported at the Apollo 12 site (6), and paleomagnetism has been found in certain Apollo 11 and Apollo 12 samples (7). For a single

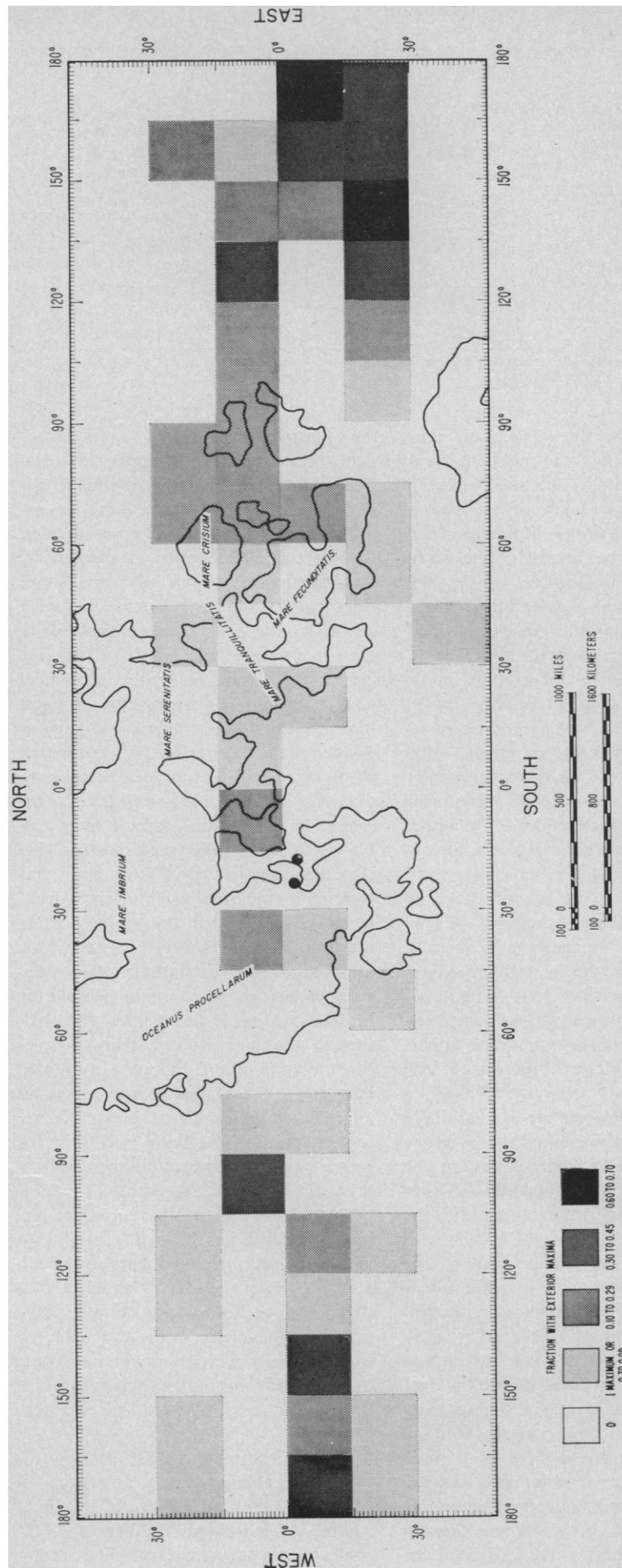


Fig. 2. Locations of sources for exterior maxima in the magnetic field magnitude, projected onto the moon's surface with use of solar wind flow directions. Fractional concentrations are presented as shaded areas, $15^\circ \times 15^\circ$, on an outline map of the equatorial regions. The darkest shading indicates the highest concentration of source locations, associated with fossil lunar magnetism or variations in crustal conductivity. Approximate locations of maria are shown also. Except for a region in the vicinity of the crater Kepler and the edge of Mare Tranquillitatis, the great maria are nearly completely excluded from the positive events. The average number of samples in each $15^\circ \times 15^\circ$ area is 12 for the 30° of latitude nearest to the equator, and 5 for the remainder of the map. Locations of the Apollo 12 and Apollo 14 surface magnetic field measurements are indicated with dots; the Apollo 12 location is the western of the two.

Table 1. Regions on the lunar surface where the concentration of source locations was tested.

Seleno-centric latitude	Seleno-centric longitude	Area ($\times 10^5$ km ²)	Fraction of observations showing anomaly*	Calculated probability that there is no concentration at the location	Nearby feature
5°–20°S	135°E–165°W	10	0.5	$\ll 10^{-5}$	Mare \bar{X} (Gagarin)
6°N	88°W	2	.4	$< 10^{-5}$	“Montes d’Alembert”
0°–20°N	60°–115°E	10	.3	3×10^{-3}	Mare Marginis
5°S	138°W	0.7	.3	6×10^{-3}	Crater 244 (Vavilov)
2°N	35°W	1	.2	$< 10^{-5}$	Encke-Kepler
5°N	0°	0.9	.1	5×10^{-4}	Pallas
0°	25°E	0.8	.1	4×10^{-5}	Delambre

* These fractions are based upon $15^\circ \times 15^\circ$ regions.

dipole lying near the surface to produce the steady background field measured at the Apollo 12 site a dipole location within 300 km of the site is required (6). This upper limit is less than the distance to the nearest of the seven regions listed in Table 1, near the craters Encke and Kepler. It is likely that the source of the Apollo 12 field is extended and diffuse if it is due to magnetized magma, and a point dipole may be only a quantitatively useful idealization. If a singular source is assumed, finite gyro radius effects (due to the temperature of the solar wind) would make a strong interaction near the source questionable; for either singular or diffuse sources some threshold based upon both scale size and field strength must be exceeded for an interaction. Detailed analysis of the Apollo 12 field suggests a scale size small relative to the ~ 400 -km upper limit of possible sizes (8). In spite of the complexities suggested by the Apollo 12 observations and the apparent lack of an interaction due to the Apollo 12 steady background field, a direct explanation of the general field of disturbances presented here is the occurrence of localized regions on the moon magnetized sufficiently (6) to create a vestigial interaction with the solar wind.

In addition, it is now known that the global electromagnetic response of the moon amplifies the incident hydro-magnetic continuum in the solar wind by a factor of about 4 at the highest frequencies examined (~ 0.04 Hz) with the Apollo 12 magnetometer, and at the subsolar point where containment of the induced field is a maximum (9). At near grazing angles, some induced magnetic field lines may be incompletely contained and thereby leak into the solar wind. A model for

the perturbations based upon transient induction would imply that the leakage of flux (and the attendant appearance of the perturbation) is associated with a thinner crust locally. In this model the crust is defined by the subsurface region of very small electrical conductivity, and the skin depth at the frequencies involved in the interaction is larger than the crustal thickness. However, geological and geochemical arguments suggest that the highlands comprise regions thicker than the maria (10), composed of material with reduced electrical conductivity by comparison with deeper rocks. An anomalous conductivity profile (11) would be required for this structure to be consistent with this electrical induction mechanism. An alternative model for the source of an intermittent interaction between the solar wind and the limb involves transient electrical induction in conducting islands in the lunar crust (12). Although the maria seem likely sources for the interaction, the data presented here favor the highlands; otherwise an anomalous conductivity profile is required, that is, one with basalts in the maria having a lower conductivity than highland material. A steady unipolar generator as a possible source for exterior maxima has been discussed (5). The data set presented here is associated with interplanetary magnetic fields that are tipped out of the ecliptic plane more than average; these data are not in agreement with a model consisting of a steady unipolar generator, for which polar regions would be well represented.

For an estimated cross section for charge exchange and deflection of 10^{-16} cm² and a scale size of 0.1 lunar radius, a neutral gas density of $\sim 10^7$ molecules per cubic centimeter at the

surface is required to deflect 1 percent of the incident solar wind flux. However, there exists no prima facie evidence that plutonic processes accompanied by gas escape are likely, especially in the highlands.

Mass concentrations that have been reported for the moon’s near side lie in the centers of ringed maria (13). In these magnetometer data, concentrations of source locations are not found in these maria, but seem to lie adjacent to most mascon locations (14), and especially on the far side, for which detailed gravimetric measurements are not yet available.

In summary, although there are a number of possible sources for the apparent limb interactions seen downstream from the limb, magnetization of selected nonmare areas, analogous to that measured by the Apollo 12 magnetometer, appears to be favored. Inductive mechanisms appear to require anomalous conductivity profiles, and an implied dependence of the response upon fluctuations in the interplanetary field has not yet been detected in the data, but we have not ruled out sources of this sort. There are no other results to indicate that sufficient gas would be present to produce the required deflection of the solar wind.

J. D. MIHALOV

C. P. SONETT

National Aeronautics and Space Administration Ames Research Center, Moffett Field, California 94035

J. H. BINSACK

Massachusetts Institute of Technology, Cambridge 02139

M. D. MOUTSOULAS

Department of Astronomy, University of Manchester, Manchester, M13 9PL, England

References and Notes

1. D. S. Colburn, R. G. Currie, J. D. Mihalov, C. P. Sonett, *Science* **158**, 1040 (1967); E. F. Lyon, H. S. Bridge, J. H. Binsack, *J. Geophys. Res.* **72**, 6113 (1967); N. F. Ness, K. W. Behannon, H. E. Taylor, Y. C. Whang, *ibid.* **73**, 3421 (1968).
2. F. C. Michel, *J. Geophys. Res.* **72**, 5508 (1967).
3. D. S. Colburn, J. D. Mihalov, C. P. Sonett, *ibid.*, in press.
4. G. L. Siscoe, E. F. Lyon, J. H. Binsack, H. S. Bridge, *ibid.* **74**, 59 (1969).
5. K. Schwartz, C. P. Sonett, D. S. Colburn, *Moon* **1**, 7 (1969); J. V. Hollweg, *J. Geophys. Res.* **73**, 7269 (1968).
6. P. Dyal, C. W. Parkin, C. P. Sonett, *Science* **169**, 762 (1970); C. W. Parkin, P. Dyal, C. P. Sonett, D. S. Colburn, *Eos* **51**, 773 (1970).
7. A. A. Levinson, Ed., *Proceedings of the Apollo 11 Lunar Science Conference* (Pergamon, New York, 1970), vol. 3, pp. 2093–2102, 2213–2219, 2305–2308, 2325–2340, 2369–2387, 2435–2451.

8. A. Barnes, P. M. Cassen, J. D. Mihalov, A. Eviatar, in preparation.
9. C. P. Sonett, P. Dyal, D. S. Colburn, B. F. Smith, G. Schubert, K. Schwartz, J. D. Mihalov, C. W. Parkin, *Transactions of the International Astronomical Union (Brighton, England)* (Reidel, Dordrecht, Netherlands, in press); C. P. Sonett, P. Dyal, C. W. Parkin, D. S. Colburn, J. D. Mihalov, B. F. Smith, *Science*, in press.
10. J. A. Wood, J. S. Dickey, Jr., U. B. Marvin, B. N. Powell, in *Proceedings of the Apollo 11 Lunar Science Conference*, A. A. Levinson, Ed. (Pergamon, New York, 1970), vol. 1, pp. 965-988; *Science* **167**, 602 (1970).
11. D. L. Lamar and J. McGann, *Icarus* **5**, 10 (1966).
12. J. V. Hollweg, *J. Geophys. Res.* **75**, 1209 (1970).
13. P. M. Muller and W. L. Sjogren, *Science* **161**, 680 (1968).
14. Recent nearside gravimetric results were kindly supplied in advance of publication by W. L. Sjogren.
15. We thank A. Barnes, P. M. Cassen, D. S. Colburn, and A. Eviatar for helpful discussions, and D. E. Wilhelms, W. L. Quaide, R. Greeley, and R. G. Strom for information about lunar topography and nomenclature.

9 November 1970

Time Scales for Lithium Depletion and Rotational Braking in Solar-Type Main-Sequence Stars

Abstract. *The new age determination of 9×10^8 years for the Hyades yields an e-folding time for lithium depletion in G dwarfs of 1.1×10^9 years and an e-folding time for rotational braking of around 2.2×10^9 years. A proposal is made that the change in solar rotation over the past 250 million years be determined by analyzing petrified trees.*

Both the lithium content and rotational velocity of solar-type main-sequence stars are known to be highest in the Pleiades, lower in the Hyades, and lowest in the sun and other apparently "old" stars in the galactic disk (1-4). This may indicate a physical connection between the braking of rotation and lithium depletion in or below the convective envelopes of solar-type stars (see 3).

Observations show (4, 5) that, within the same star cluster, the K dwarfs generally have a much lower lithium content than the G dwarfs, which indicates that lithium is depleted faster in stars of small mass than in the more massive stars. For this reason, to obtain the time scale for lithium depletion for a certain type of stars, we should compare only stars of similar spectral type but of different age. One of us (P.S.C.) made this comparison, using an age of 4×10^8 years for the Hyades and a solar lithium abundance of 2.4 (scale: hydrogen abundance = 10^{12} ; this scale will be used throughout this report); it was found that the e-folding times for rotational braking and lithium

depletion derived from the ages of the Hyades and Pleiades predict a solar rotational velocity and lithium content about two orders of magnitude lower than the observed values.

We wish to point out here that with the new age determination of 9×10^8 years for the Hyades (6) the lithium content of solar-type stars as a function of time fits an exponential decay law with an e-folding time of 1.1×10^9 years. Furthermore, an exponential decay law with an e-folding time of about 2.2×10^9 years gives a reasonable fit for the braking of rotation. The observations and the two exponential laws

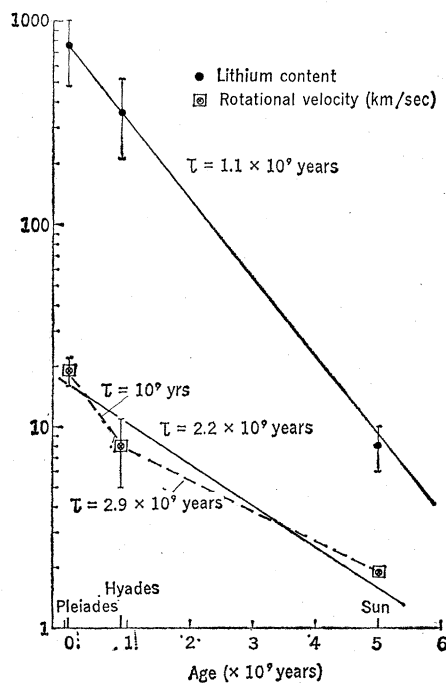


Fig. 1. Lithium contents [after Conti (3), Engvold *et al.* (7), and Müller (8)] and rotational velocities [after Kraft (2)] as a function of age for G-type main-sequence stars, together with best fitting exponentially decreasing functions. For the rotational velocities, two possible braking laws are represented; one with a uniform e-folding time over the entire interval of 5×10^9 years, the other with rapid braking for the first 10^9 years, and slower braking later.

mentioned above are represented in Fig. 1. Observed values of the lithium content in G stars in the Pleiades and Hyades were taken from Conti's paper (3). The solar lithium content of 8.0 ± 2.0 is the average of the two most recently revised values for this quantity (7, 8).

The error bars for the lithium contents are based on the observational spread in lithium abundance for G stars in the respective clusters. The observed rotational velocities of G stars in the Pleiades and Hyades were taken from Kraft (2). Possible errors in Kraft's determinations of the rotational velocities are estimated to be about ± 3 km/sec. It can be seen in Fig. 1 that, within the observational error limits, the exponential decay laws provide a good fit to the observations for the Pleiades, Hyades, and the sun.

According to the best fitting exponential function through the values for the Pleiades and Hyades, the presently expected solar lithium content is 9, in close agreement with the observed value. For the rotation the situation may be somewhat more complex. The dashed lines show that a possible alternative interpretation for the slowing down of rotation may be an e-folding time of about 10^9 years for the first 10^9 years and, subsequently, an e-folding time of 2.9×10^9 years. The uncertainties in the rotational velocities are such that both interpretations are possible. If we assume that the exponential with an e-folding time of 2.2×10^9 years represents the real slowing-down law, the presently expected solar equatorial velocity of rotation becomes 1.6 km/sec, which is close to the observed value of 1.91 km/sec (9).

There may be a simple way to determine the slowing down of solar rotation over the past 200 to 250 million years by measuring the variations in thickness of growth rings in petrified trees. Because the thickness of rings in present-day trees shows a correlation with the sunspot cycle (10), such tree-ring data are expected to yield the period of solar activity in the past. The length of this period is expected to be inversely proportional to the solar equatorial velocity of rotation at that epoch, for the following reason. According to the observations (11) the solar angular velocity of rotation as a function of the latitude ϕ can be described by the formula

$$\Omega = \Omega_0 (1 - 0.19 \sin^2 \phi) \quad (1)$$